Magnetic Resonance in Medicine

3D MR Fingerprinting for Dynamic Contrast-Enhanced Imaging of Whole Mouse Brain

Yuran Zhu[1], Guanhua Wang[2], Yuning Gu[1], Walter Zhao[1], Jiahao Lu[1], Junqing Zhu[3], Christina J. MacAskill[1], Andrew Dupuis[1], Mark A. Griswold[1,3], Dan Ma[1,3], Chris A. Flask[1,3,4], Xin Yu[1,3,5]

[1]Department of Biomedical Engineering, Case Western Reserve University, Cleveland, Ohio, USA
[2]Department of Biomedical Engineering, University of Michigan, Ann Arbor, Michigan, USA
[3]Department of Radiology, Case Western Reserve University, Cleveland, Ohio, USA
[4]Department of Pediatrics, Case Western Reserve University, Cleveland, Ohio, USA
[5]Department of Physiology and Biophysics, Case Western Reserve University, Cleveland, Ohio, USA

Address correspondence to:

Xin Yu, Sc.D.,
Wickenden 430
10900 Euclid Avenue
Cleveland, OH 44106, USA
Tel: 216-368-3918
Email: xin.yu@case.edu

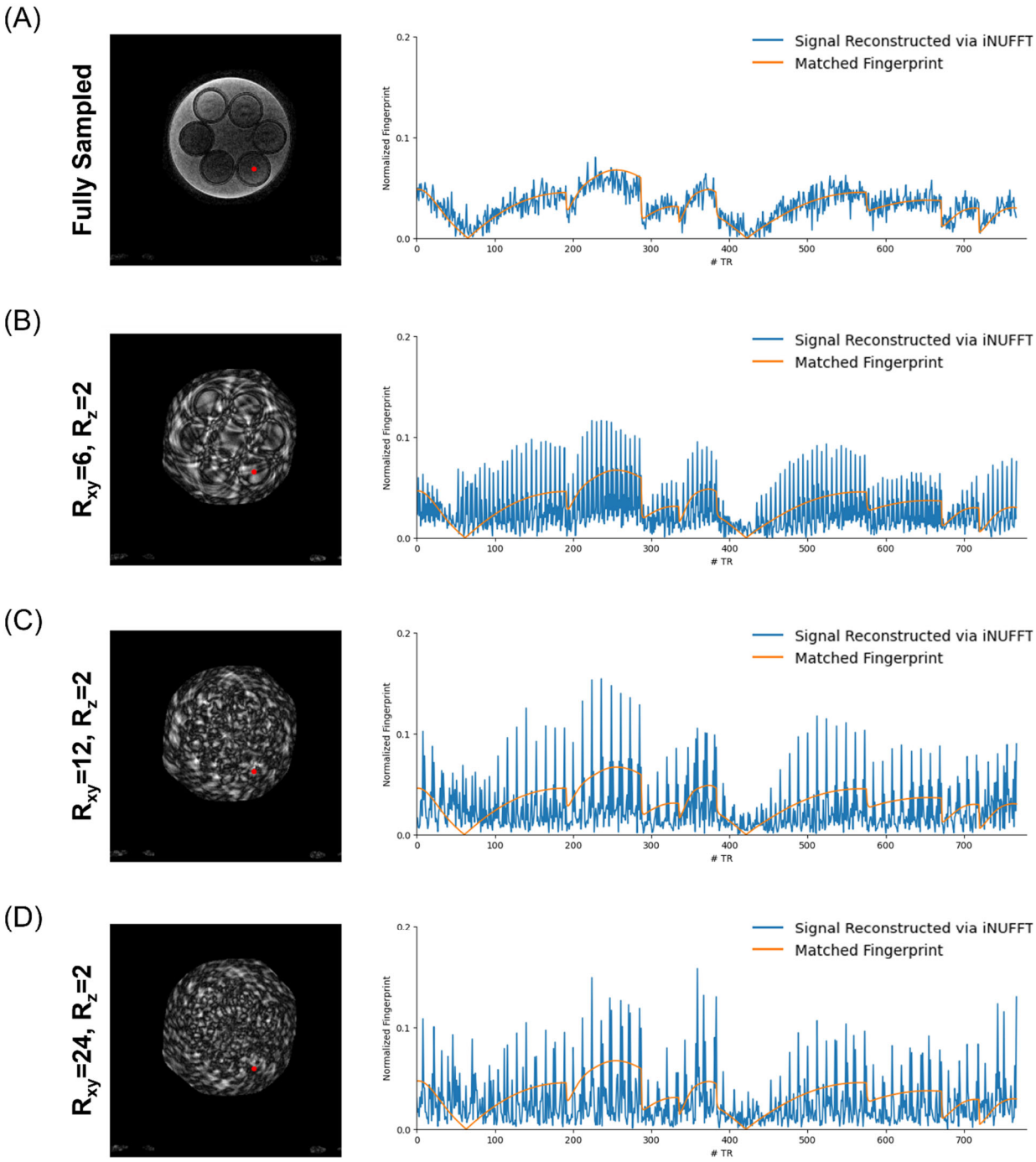


FIGURE S1. Representative images of the 12th frame of an in vitro MRF dataset (left) and the corresponding fingerprints and matched dictionary entries from the voxel highlighted in red (right) from fully sampled (A) and undersampled (A-D) data. R_{xy} and R_z are the in-plane and through-plane undersampling factors, respectively.

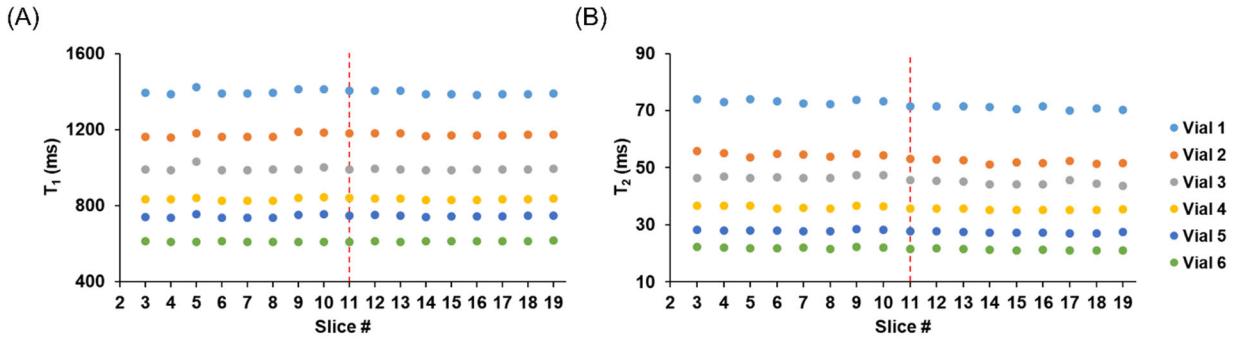


FIGURE S2. Comparison of inter-slice variations in MRF-measured T_1 (A) and T_2 (B) values in six phantom vials. Red dotted lines indicate the center slice.

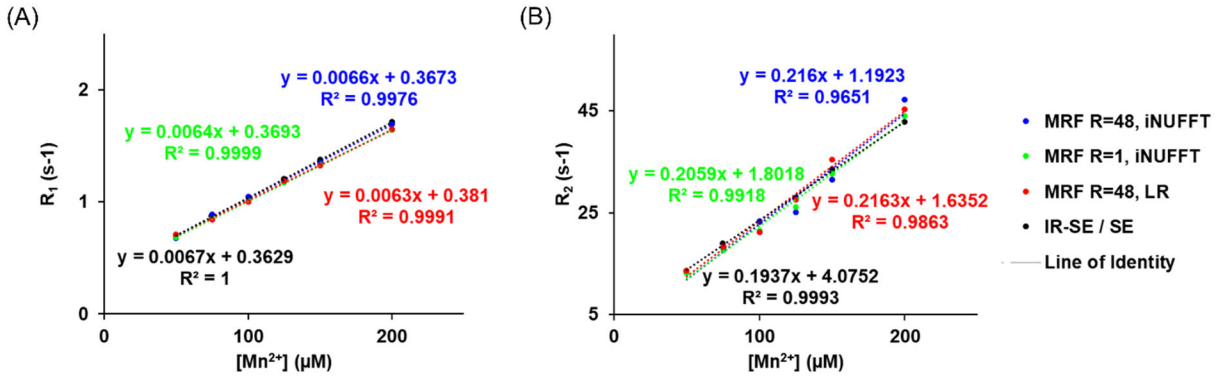


FIGURE S3. Correlation of relaxation rates and Mn^{2+} concentrations. (A) Correlation of Mn^{2+} concentration and R_1 derived from 3D MR fingerprinting (MRF) and inverse-recovery spin echo (IR-SE) methods. (B) Correlation of Mn^{2+} concentration and R_2 derived from MRF and spin-echo (SE) methods.

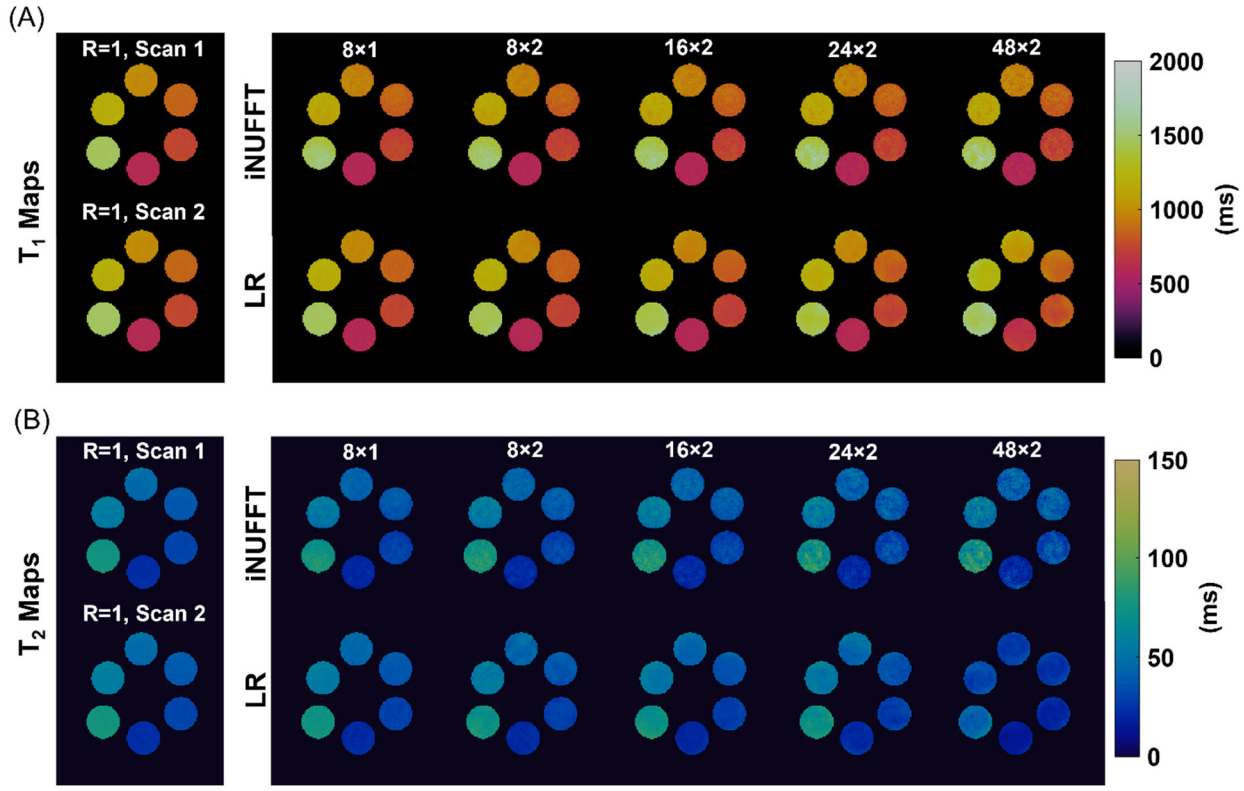


FIGURE S4. T_1 and T_2 results from fully sampled and undersampled MR fingerprinting (MRF) scans. (A) T_1 maps from two fully sampled MRF scans and those from undersampled scans with varied in-plane (R_{xy}) and through-plane (R_z) undersampling factors, reconstructed with inverse non-uniform Fourier transform (iNUFFT) and low-rank (LR) subspace modeling. (B) T_2 maps from two fully sampled MRF scans and those from undersampled scans with varied R_{xy} and R_z undersampling factors, reconstructed with iNUFFT and LR.

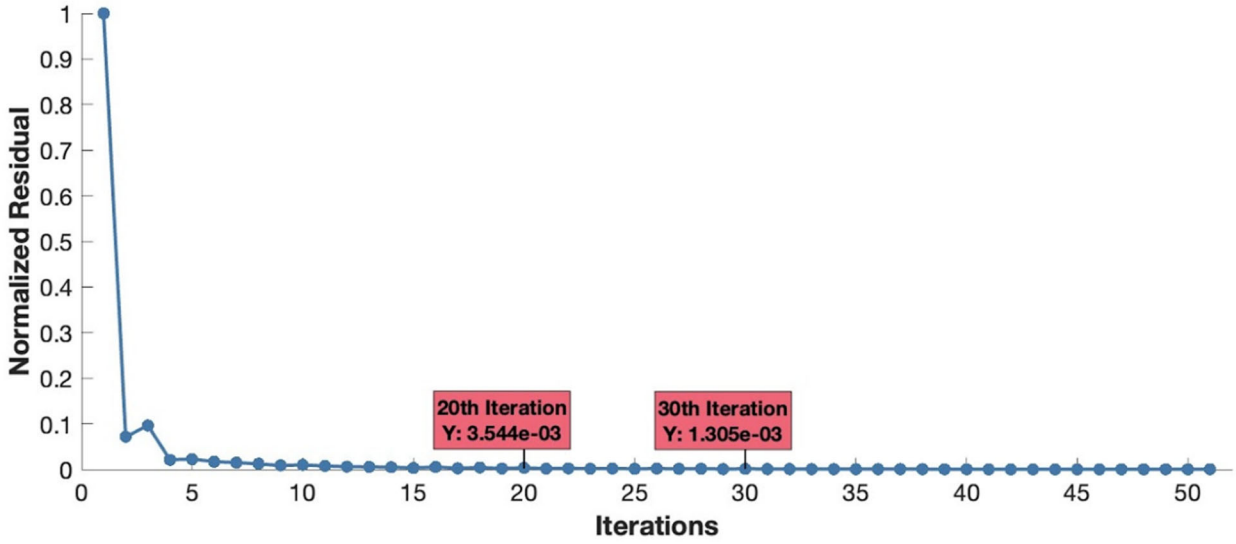


FIGURE S5. Normalized residuals over conjugate gradient (CG) iterations for subspace-based image reconstruction via low rank (LR) for MR fingerprinting (MRF) acquired at 48-fold undersampling. Normalized residual is defined as $\left|\left|A\hat{U}\hat{V}-y\right|\right|/\left|\left|y\right|\right|$.

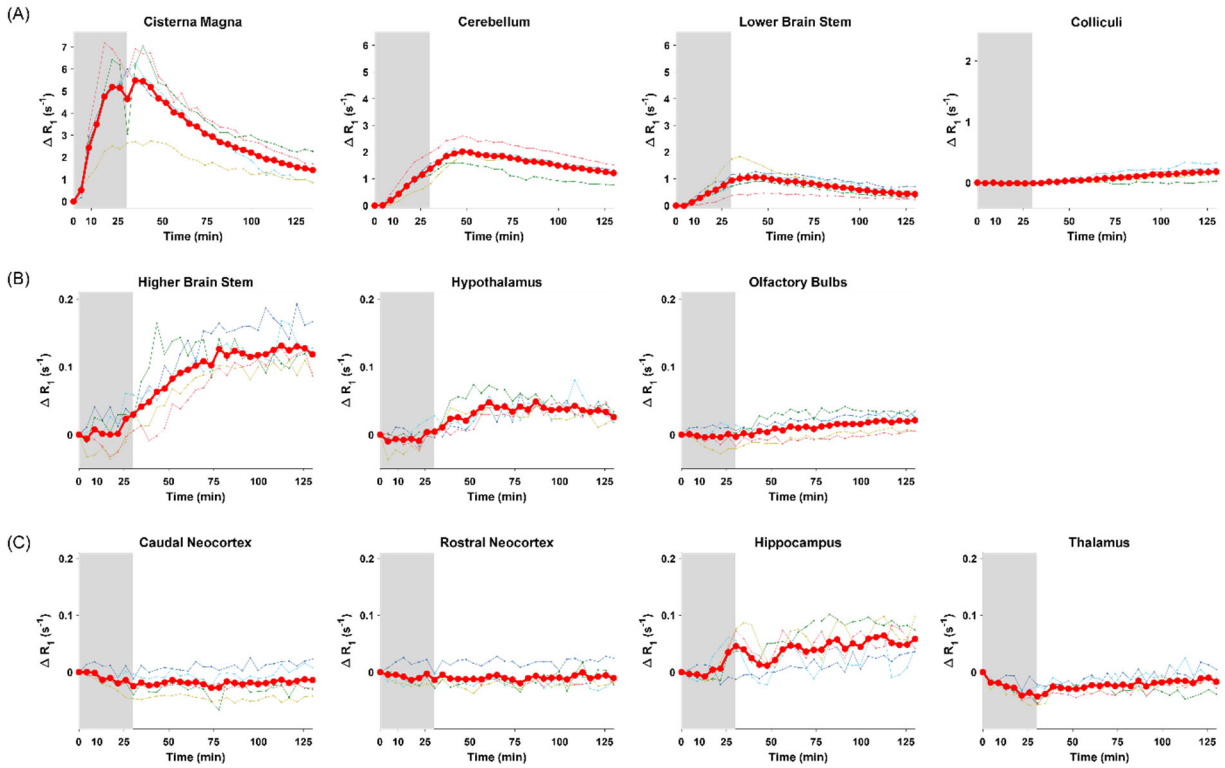


FIGURE S6. Time courses of ΔR_1 changes in selected ROIs following Gd-DTPA infusion at cisterna magna. (A) Proximal to the infusion site. (B) Along the ventral brain surface. (C) Along the dorsal brain surface and in the deep brain. The individual animal data (n = 5) are plotted as thin lines, and the mean data are plotted as thick red lines. Shaded areas represent standard errors.

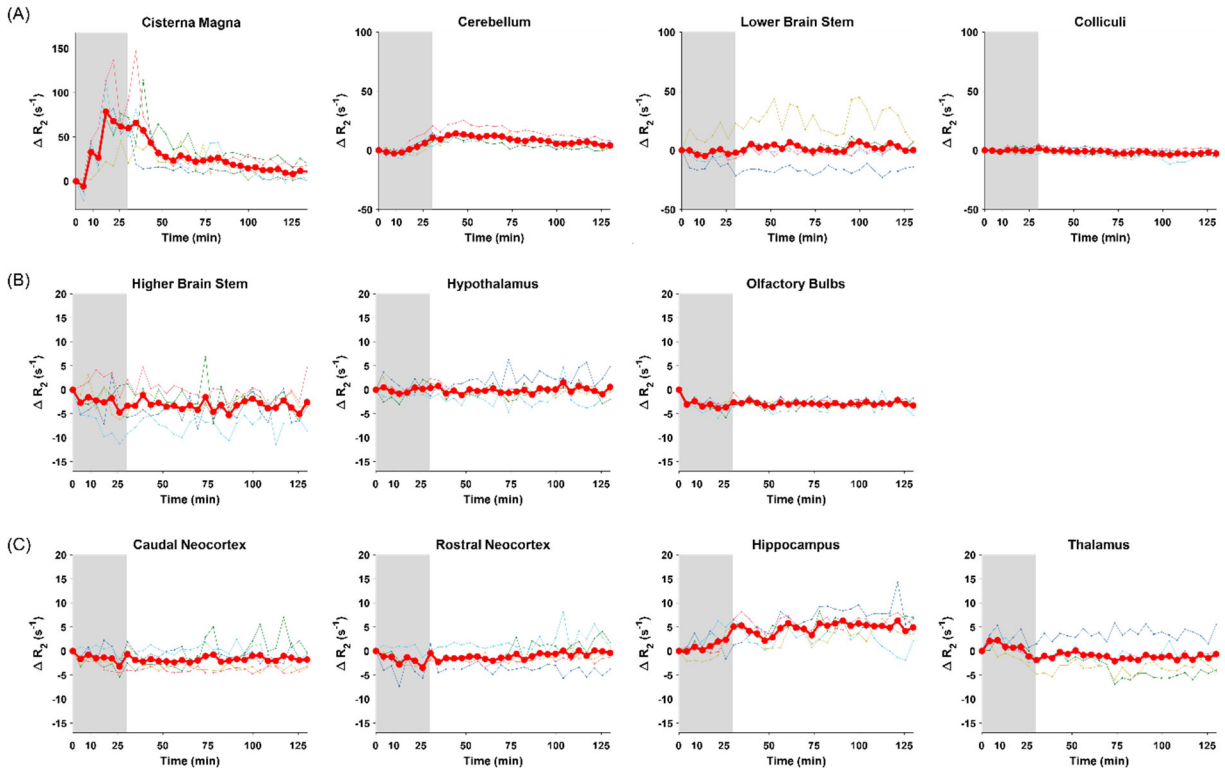


FIGURE S7. Time courses of ΔR_2 changes in selected spherical volumes placed at different brain regions following Gd-DTPA infusion at cisterna magna. (A) Proximal to the infusion site. (B) Along the ventral brain surface. (C) Along the dorsal brain surface and in the deep brain. The individual animal data (n = 5) are plotted as thin lines, and the mean data are plotted as thick red lines. Shaded areas represent standard errors.